

Chemical sensing by differential thermal analysis with a digitally controlled fiber optic interferometer

L. C. Gonçalves, G. González-Aguilar, O. Frazão, J. M. Baptista, and P. A. S. Jorge

Citation: *Rev. Sci. Instrum.* **84**, 015002 (2013); doi: 10.1063/1.4774054

View online: <http://dx.doi.org/10.1063/1.4774054>

View Table of Contents: <http://rsi.aip.org/resource/1/RSINAK/v84/i1>

Published by the [American Institute of Physics](http://www.aip.org).

Related Articles

Experimental approach to the microscopic phase-sensitive surface plasmon resonance biosensor
Appl. Phys. Lett. **102**, 011114 (2013)

Porous silicon micro- and nanoparticles for printed humidity sensors
Appl. Phys. Lett. **101**, 263110 (2012)

Advance in multi-hit detection and quantization in atom probe tomography
Rev. Sci. Instrum. **83**, 123709 (2012)

Giant enhancement of H₂S gas response by decorating n-type SnO₂ nanowires with p-type NiO nanoparticles
Appl. Phys. Lett. **101**, 253106 (2012)

Hydrogen gas sensor based on palladium and yttrium alloy ultrathin film
Rev. Sci. Instrum. **83**, 125003 (2012)

Additional information on *Rev. Sci. Instrum.*

Journal Homepage: <http://rsi.aip.org>

Journal Information: http://rsi.aip.org/about/about_the_journal

Top downloads: http://rsi.aip.org/features/most_downloaded

Information for Authors: <http://rsi.aip.org/authors>

ADVERTISEMENT



**Does your research require low temperatures? Contact Janis today.
Our engineers will assist you in choosing the best system for your application.**



10 mK to 800 K **LHe/LN₂ Cryostats**
Cryocoolers **Magnet Systems**
Dilution Refrigerator Systems
Micro-manipulated Probe Stations

sales@janis.com **www.janis.com**
Click to view our product web page.

Chemical sensing by differential thermal analysis with a digitally controlled fiber optic interferometer

L. C. Gonçalves,^{1,2} G. González-Aguilar,² O. Frazão,² J. M. Baptista,^{1,2} and P. A. S. Jorge²

¹*Centro de Ciências Exactas e da Engenharia, Universidade da Madeira, 9300-390 Funchal, Portugal*

²*INESC Porto, Rua do Campo Alegre, 687, 4169-007 Porto, Portugal*

(Received 5 October 2012; accepted 16 December 2012; published online 8 January 2013)

In this work the implementation of an optical fiber interferometric system for differential thermal analysis enabling the identification of chemical species is described. The system is based on a white light Mach-Zehnder configuration using pseudo-heterodyne demodulation to interrogate two identical fiber Bragg gratings (FBG) in a differential scheme. System performance is compared using either standard hardware or low cost virtual instrumentation for operation control and signal processing. The operation with the virtual system enabled temperature measurements with a ± 0.023 °C resolution nearly matching the performance of the standard hardware. The system ability to discriminate chemical species by differential thermal analysis was demonstrated. Mixed samples of acetone and methanol could be successfully identified, indicating the suitability of the system for high precision measurements using low cost instrumentation. © 2013 American Institute of Physics. [<http://dx.doi.org/10.1063/1.4774054>]

I. INTRODUCTION

The measurement of temperature differentials allows the implementation of highly sensitive techniques that can be used to assess absorption or release of energy involved in chemical processes. Techniques such as thermogravimetry, differential thermal analysis, and differential scanning calorimetry are in widespread use as material characterization techniques in different fields of activity.¹ In particular, these methods can be used as confirmation techniques for determination of the composition of unknown samples in various applications ranging from chemical analysis to explosive detection.²

In this context, the use of optical fiber sensors as sensing elements of temperature is quite attractive. Immunity to electromagnetic interference, high sensitivity, miniaturization, low cost, ease of implementation of differential configurations, possibility of remote interrogation, and multiplexing ability are some of the advantages associated with this technology. The application of optical fiber calorimeters has been demonstrated in demanding military applications where a Michelson interferometer with a difference of optical paths of 1.6 km, allowed the authors to achieve a dynamic range $> 10^9$ and a temperature resolution of $\pm 10^{-8}$ °C. The system was used in the characterization of radioactive materials.³ In a different application, a differential white light interferometric configuration using two Hi-Bi fiber loop mirrors, and signal analysis in the spectral domain was used to measure laser emission power, up to 3 W with a 0.3 mW resolution.⁴

In this context, the use of more advanced signal processing techniques such as white light interferometry and pseudo-heterodyne detection systems enable coherence tuning, improved sensitivity, and higher dynamic range.⁵ Such features are highly attractive and have been explored in applications requiring real time monitoring of physical, biological, and

chemical parameters.⁶ In particular, when used in a differential configuration, these interferometric techniques have a strong potential to be explored in high sensitivity thermal analysis methods.⁷ Kersey *et al.* reported a differential configuration where a white light Mach-Zehnder interferometer was used to interrogate a pair of fiber Bragg gratings (FBG) achieving a resolution better than 0.05 °C.⁸ The use of differential interferometric systems is widely explored in different fields of application. However, it is common that such systems are associated with bulky configurations using expensive equipments. Nevertheless, these schemes are very attractive because they have a high sensitivity, high dynamic range, and are immune to power fluctuations that might occur in the lead-in optical fibers. In order to exploit the advantages of the interferometric interrogation systems while minimizing the downsides, virtual instrumentation is an attractive solution that enables cost reduction by replacing some of the physical instruments by virtual instruments, and also facilitating signal processing and data storage and analysis.⁹

Meggitt *et al.*¹⁰ presented a digital phase tracking algorithm for fiber Bragg grating sensor for measuring strain and temperature with high sensitivity eliminating phase ambiguity. In this particular case, however, the digital system was used only for signal acquisition and processing and did not control the full system.

In the work here presented, an interferometric system, fully controlled with virtual instrumentation developed in LabVIEW[®] environment, is described for chemical sensing by differential thermal analysis. A Mach-Zehnder white light system is used to interrogate two FBGs in a differential arrangement. System performance and calibration is performed, measuring temperature and strain, using both standard hardware and virtual instrumentation. Finally the identification of mixed chemical samples in a digitally controlled differential thermal analysis setup is demonstrated.

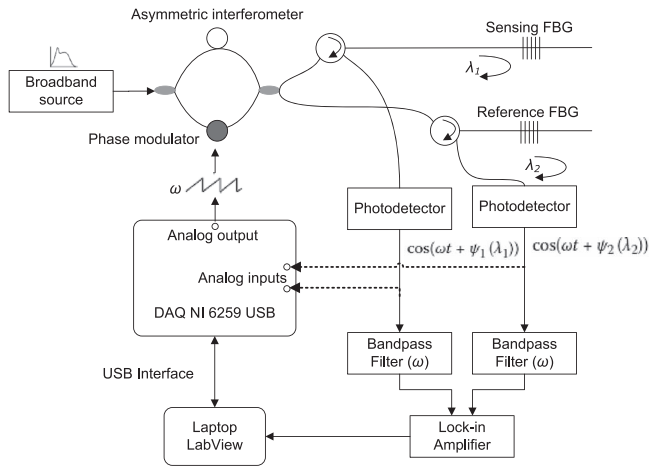


FIG. 1. The experimental scheme implemented.

II. EXPERIMENTAL SETUP

The implemented experimental scheme uses a receiving interferometer to interrogate two FBG sensors and is shown in Figure 1. The system is based on a fiber optic Mach-Zehnder interferometer using two couplers with a 50/50 coupling ratio and is illuminated with a depolarized broadband erbium doped fiber source to minimize birefringence induced drift and noise.¹¹ The optical signal can be phase modulated, using an electro-optic modulator (APE from JSDU) in one of the arms of the interferometer. In the other interferometer arm, an adjustable air path was implemented using GRIN lens, which allowed adjusting the interferometer optical paths imbalance. In this particular application, a pseudo-heterodyne scheme was applied, where the interferometer phase was modulated with a sawtooth waveform ($f = 1$ kHz), with its amplitude adjusted to obtain a 2π phase excursion. In these conditions, an electronic carrier is generated at the interferometer output, whose phase depends on the wavelength of the sensing FBGs.

In particular the two Mach-Zehnder outputs will produce two out-of-phase signals that can be analyzed in a differential scheme. In this case, the phase difference between the two signals cancels out all environmental noise affecting the interrogation interferometer, and depends only on the wavelength of the FBGs. In each of the gratings, the temperature induced shift in the Bragg wavelength, causes a phase change given by

$$\Delta\Phi = -\frac{2\pi n \Delta L}{\lambda_B^2} \Delta\lambda_B, \quad (1)$$

where $\Delta\Phi$ is the phase variation, n is the fiber refractive index, ΔL is the interferometer path imbalance, λ_B is the Bragg wavelength of the grating, and $\Delta\lambda_B$ is the change induced in the Bragg wavelength by the measurand. When this change is caused by a temperature variation ΔT is given by:

$$\Delta\lambda_B = \frac{\partial\lambda_B}{\partial T} \Delta T. \quad (2)$$

In practice, at the output of the system, two photodetectors collected the signals reflected by each FBG: two sine waves with the same frequency, ω , but with a relative phase proportional to their wavelength difference.

Using one of the FBG as a reference and the other as the operational sensor, very accurate measurements can be made by tracking the relative phase of the two interferometer outputs. For this purpose, these signals were either feed into a lock-in amplifier (SR530 from SRS) or into the analog inputs of a digital acquisition board (NI-USB-6259) and processed using LabVIEW. Signal processing involved the amplification and filtering of the signals for subsequent detection of the phase difference which was obtained by Fourier transform. In both cases the data acquisition (DAQ) board was also used to control the phase modulator. In this way the system was fully controlled by the digital system.

Prior to the implementation of the chemical sensing setup, the interferometric system performance was tested and compared using the hardware (Lock-in) and the virtual system (DAQ and software) to retrieve the relative phase of the outputs. To assess the influence of the FBG relative wavelengths, both systems were tested using a pair of FBGs with identical wavelengths and a pair of FBGs with different wavelengths.

The software developed in LabVIEW allowed the implementation of the pseudo-heterodyne detection scheme, as well as the acquisition and processing of the photodetector signals. The software developed allowed full control of the amplitude and the frequency of the modulation signal and adjustment of the sample rate of the signals acquired by the DAQ. The experimental conditions were set to have a modulation pseudo-heterodyne amplitude of 7 V with a frequency of 1 kHz and a sample rate of 10 kHz. The phase modulator had a bandwidth in the MHz range; therefore, these operational parameters ensured that the fly-back effect and its induced phase errors were minimized.¹²

The virtual system implemented for phase recovery was based on the Fourier transform of the interferometer output signals. The signals acquired using a DAQ were sampled with a rate proportional to the frequency of the modulation signal. This condition guarantees the acquisition of a quasi-sinusoidal signal in the output. After filtering, the Fourier transform of the sinusoidal signal in the output is given by

$$\cos(\omega_0 t + \varphi) \xrightarrow{F} \pi e^{j\varphi} \delta(\omega - \omega_0) + \pi e^{-j\varphi} \delta(\omega + \omega_0). \quad (3)$$

Once the Fourier transform was calculated, the phase difference between reference and sensor signals was easily retrieved. Figure 2 shows the acquired signals in the front panel of the software developed.

The signals at the left side are unprocessed (their dc component was removed) and as acquired by the DAQ. Their amplitudes were subsequently equalized prior to the application of the Fourier transform operation in order to ensure stable phase retrieval (signals at the right side).

III. RESULTS AND DISCUSSION

To validate and optimize the system operation, a set of experimental tests was performed to evaluate the system response to temperature and strain. In all cases regression analysis was performed from which sensitivity and resolution were

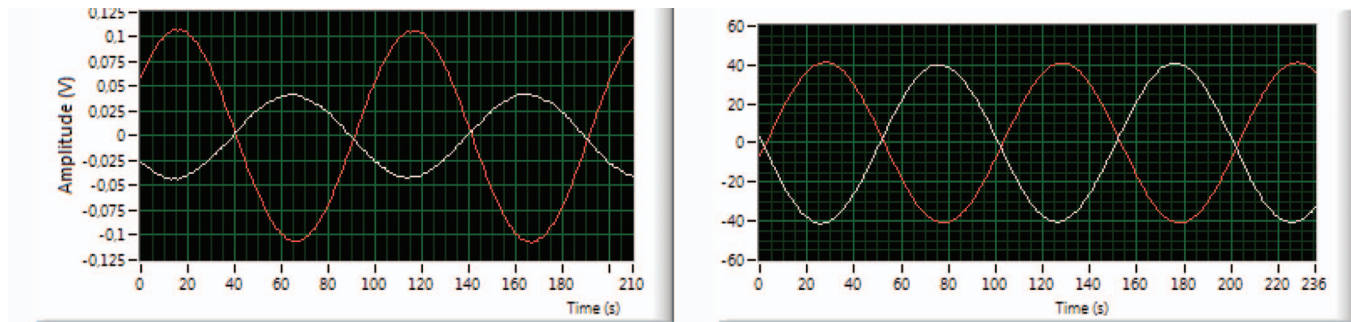


FIG. 2. Signals processed by the LabVIEW application.

assessed. Maximum relative errors were estimated from the statistics and represented as error bars.

Strain measurements were initially performed. For this purpose, one of the FBGs was placed and glued on two supports that were located 0.51 m apart like it is shown in Figure 3. One of the supports was attached to a precision translation stage that stretched the fiber up to 1 mm in steps of 100 μm . The second FBG was kept at a constant stretch and was used as a reference.

The relative phase of the Mach-Zehnder outputs was registered for different values of applied strain using both the hardware and the virtual interrogation systems. The resulting phase values as function of the applied strain are presented in Figure 4, for both cases when a pair of identical FBGs was used as sensor and reference element.

The results obtained demonstrate that the virtual system has a response very similar to the configuration implemented using standard instrumentation. In both cases the use of standard unwrapping algorithm allowed to eliminate the 2π phase ambiguity, enabling the extension of the dynamic range to thousands of degrees. The sensitivity obtained with standard instrumentation was of $0.82^\circ/\mu\epsilon$ while for the virtual instrumentation a value of $0.78^\circ/\mu\epsilon$ was recorded. On the other hand, resolutions of $\pm 487.80 \text{ n}\epsilon$ and $\pm 589.74 \text{ n}\epsilon$ were obtained with the hardware and the virtual systems, respectively. These values were calculated from the standard deviation of the measured phase signals over intervals exceeding 10 min, demonstrating the system stability and the effectiveness of the differential detection scheme. The fact that the sensor and the reference FBGs used had similar or distinct wavelengths had practically no impact on the system performance. This fact can be confirmed in Figure 5 and Table I where results obtained for strain measurements using FBGs with identical (1550 nm) or distinct wavelengths (1550 nm and 1545 nm) are displayed.

It was verified that the standard deviation of the measured phase was very small and identical in both cases. These results indicate that common noise rejection of the differential scheme was very effective and was not affected by the FBG's wavelengths.

IV. TEMPERATURE TESTS

The scheme of the differential thermal analysis setup is shown in Figure 6. For the temperature measurement, the reference grating was kept unstrained at a constant temperature of 0°C by immersion in water and ice. The sensor grating, on the other hand, was subjected to temperature variations using a Peltier element controlled by LabVIEW. In order to calibrate the system, a precalibrated thermistor was used as a reference. The relative phase was then acquired simultaneously with the resistance value of the thermistor, as temperature was changed.

In order to evaluate the system performance using interrogation with the hardware and the virtual instrumentation, the temperature calibration curves were compared in the range 21°C – 29°C . In this case a pair of identical gratings was used. Figure 7 shows the calibration curves obtained for the temperature response of the system using standard instrumentation and virtual instrumentation.

The sensitivity obtained with the system implemented with standard instrumentation was of $20.00^\circ/\text{C}$. On the other hand, using the virtual instrumentation, a sensitivity of $19.60^\circ/\text{C}$ was attained. The resolution was estimated to be of $\pm 0.020^\circ\text{C}$ and $\pm 0.023^\circ\text{C}$, for the hardware and the virtual systems, respectively.

Considering the final application, a calibration was performed in the full range of operation of $\sim 20^\circ\text{C}$ to $\sim 75^\circ\text{C}$. The calibration procedure was repeated using a pair of identical gratings, as well as a pair of FBG with distinct

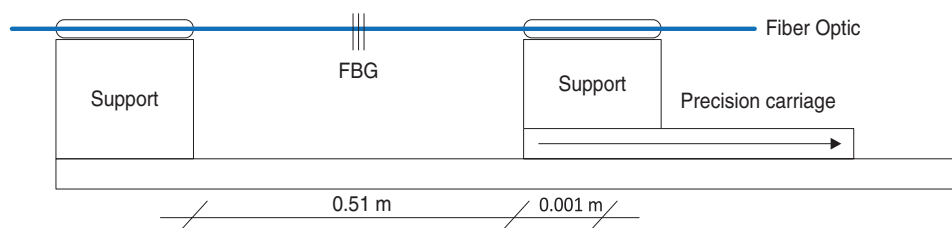


FIG. 3. Scheme of the experimental setup to apply strain to the FBG.

TABLE I. Results of strain measurements.

Wavelengths (nm)	Standard deviation 2σ (deg)	Sensitivity (deg/ $\mu\epsilon$)	Resolution (n ϵ)
1550-1545	0.46	0.780	590
1550-1550	0.46	0.778	591

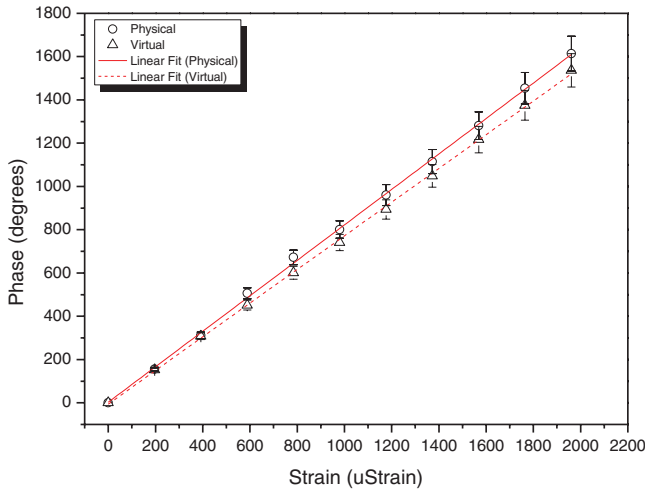


FIG. 4. Results of relative phase as function of the applied strain for both hardware and virtual implementation using a pair of identical FBGs.

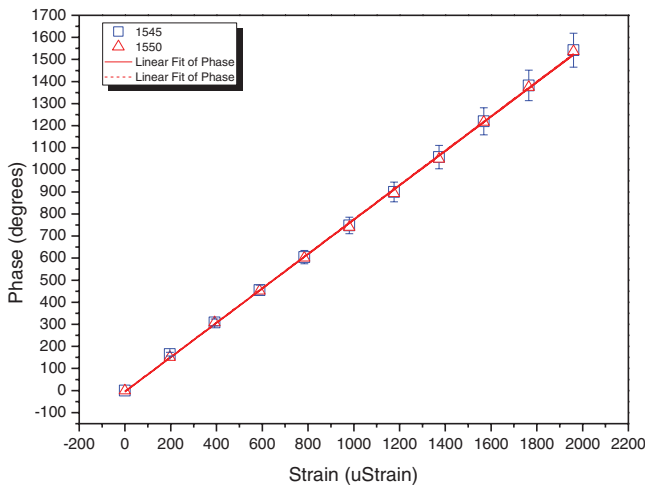


FIG. 5. Response of the system relative phase to applied strain using FBGs with identical or distinct wavelengths.

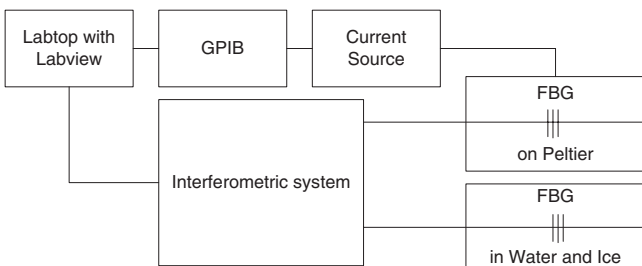


FIG. 6. Scheme of the differential temperature measurement setup.

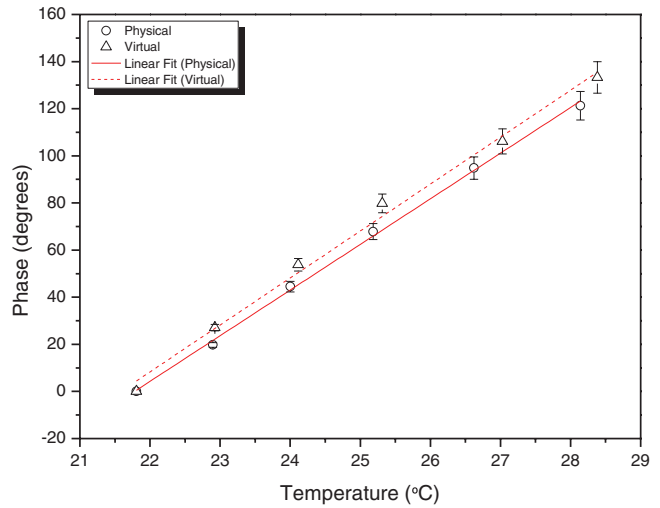


FIG. 7. Calibration curves obtained for the temperature response of the system using standard instrumentation and virtual instrumentation.

wavelengths. Very similar results could be obtained in both cases that are shown in Figure 8.

Table II shows the values of sensitivity and resolution obtained for temperature when using pairs of identical (1550 nm) or distinct (1550 nm and 1545 nm) FBGs.

Again, similar results were obtained in both cases showing that the system will allow some versatility in the choice of the FBGs' wavelength without compromising its performance. In particular standard deviation of the measure phase was identical in both cases, showing that the effectiveness of the noise rejection scheme was maintained. The small differences in sensitivity to temperature, on the other hand, may be ascribed to small differences in the thermal contact of the sensor with the sample and test chamber. Nevertheless, in both cases the system performance is identical.

Overall, resolutions were attained, $\sim 0.02^\circ\text{C}$, that are an order of magnitude larger than the standard temperature resolution obtained with spectrally interrogated FBG which is typically around 0.1°C .

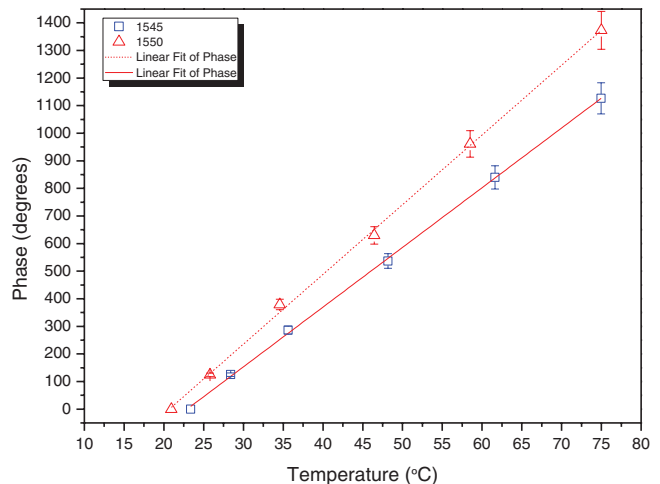


FIG. 8. Calibration curves obtained for temperature using a pair of identical FBGs (1550 nm) and a pair of distinct FBGs (1545 nm and 1550 nm).

TABLE II. Results of temperature measurements.

Wavelengths (nm)	Standard deviation 2σ (deg)	Sensitivity (deg/ $^{\circ}$ C)	Resolution ($^{\circ}$ C)
1550-1545	0.46	21.64	0.021
1550-1550	0.46	25.27	0.018

V. DIFFERENTIAL THERMAL ANALYSIS

Following the system characterization and calibration, its target application in a differential thermal analysis setup was finally tested aiming the identification of chemical substances.

For this purpose, the reference FBG was kept at 0° C while the sensor FBG was placed in a small aluminum chamber. The small sample box was placed in thermal contact with a Peltier element enabling the control of its temperature. Using a current source controlled by LabVIEW it was possible to apply a linear temperature gradient to the samples inside the test box. A rate of change of 5 mA/s in the current going through the Peltier, corresponded to a rate of temperature change inside the chamber of 0.09° C/s (linear correlation factor of 98%) and was used in the performed tests.

For the first experiment, 0.1 ml of acetone were placed inside the test chamber, on top of the sensor FBG, and then the temperature was incremented up to 66.00° C while the differential phase output of the system was recorded. The linear increment in temperature was successfully recorded up to the point where the ebullition of acetone was attained. In fact, a sudden decrease in the differential phase was registered when the temperature reached $\sim 62.13^{\circ}$ C. This happened, because the evaporation of acetone had a cooling effect on the FBG. The temperature registered for the acetone evaporation presented an offset from the theoretical value (56.53° C). This discrepancy can be due to the relatively high volume of the heating chamber when compared with the sample volume. In addition, this measurement is also influenced by the gradient of the heating ramp used throughout the experiment and can be compensated with proper calibration.¹³

In a second experiment, the process was repeated but using a mixed sample of acetone and methanol, (0.1 ml of each) and the temperature was incremented up to 74.98° C. Again, in the vicinity of the ebullition temperatures of each element of the sample sudden decreases in the temperature of the FBG were registered. Figure 9 shows the results obtained in the temperature range of interest.

Sudden decreases in the relative phase were registered at $\sim 62.16^{\circ}$ C and 70.16° C, which could be ascribed to the presence of acetone and methanol, respectively. Again, offsets from the theoretical values (56.53° C and 64.70° C, respectively) were observed. The value of the offsets is almost the same in both cases and approximately, 5.55° C, confirming a systematic deviation that can be corrected by proper calibration and control of sample/chamber volume ratio and rate of temperature change.

As expected, although the amount of samples was identical, the phase variations recorded were different in magnitude indicating different temperature variations. This occurs because each sample has different mass and heat capacity,

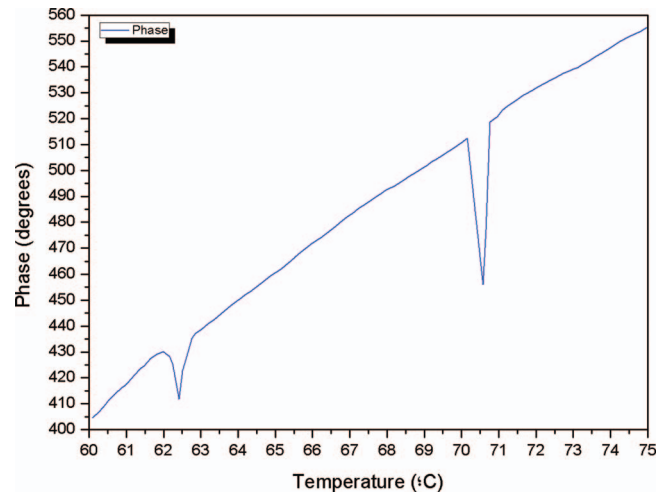


FIG. 9. Differential phase response of the system when a temperature ramp was applied to a mixed sample of acetone and methanol.

factors that directly impact the amount of absorbed or released heat in a given physical process.¹⁴ Therefore, the results obtained demonstrate the viability of the system presented to be used in the identification of unknown samples. To obtain an analytical instrument, however, several improvements are in order. Pressure inside the sample chamber needs to be known/controlled. In such case the areas of the dips in Figure 9 are proportional to the enthalpy of the vaporization reaction and can be used for quantification purposes.

Further improvements are also possible in the optical system. Using an FBG Fabry-Perot cavity instead of a simple grating can increase the intrinsic temperature sensitivity. In addition, the phase modulator used introduces birefringence in the reading interferometer that can cause some phase noise.¹¹ Introducing a depolarizer at its output may reduce significantly the phase noise, enabling higher precision.

VI. CONCLUSION

An interferometric interrogation scheme for differential thermal analysis was implemented using FBGs as temperature sensors. The system was tested using both traditional and virtual instrumentation. Differential measurements of temperature and strain were carried out and it was demonstrated that the sensitivities and resolutions obtained using the hardware and the virtual systems were nearly matched. Such results confirm that the virtual instrumentation is a valid tool to implement high performance interferometric systems at low cost. The viability of the system to be used in the identification and quantification of unknown samples through the application of differential thermal analysis was demonstrated using mixed samples of acetone and methanol. System performance can be improved by optimization of the test chamber engineering, enabling more demanding applications such as explosive detection. In addition, the application of the interrogation setup to monitor other quasi-static measurands, such as refractive index, has a strong potential for biosensing applications.

ACKNOWLEDGMENTS

This work was supported by “Fundação para a Ciência e Tecnologia” AQUAMONITOR - PTDC/AAC-AMB/112424/2009 (FCOMP_01-0124-FEDER-013911).

¹M. I. Brown, *Introduction to Thermal Analysis Techniques and Applications* (Kluwer Academic, Netherlands, 2001).

²Y. S. Liu, V. M. Ugaza, S. W. North, W. J. Rogers, and M. S. Mannana, *J. Hazard. Mater.* **142**, 662–668 (2007).

³P. Davis, S. Bayliss, and C. Rudy, *Proc. SPIE* **3860**, 400–406 (1999).

⁴A. V. Khomenko, A. García-Weidner, J. Tapia-Mercado, and M. A. García-Zárate, *Opt. Commun.* **198**(1-3), 29–35 (2001).

⁵Y. J. Rao and D. A. Jackson, *Meas. Sci. Technol.* **7**, 981–999 (1996).

⁶C. Jesus, S. F. O. Silva, M. Castanheira, G. González-Aguilar, O. Frazão, P. A. S. Jorge, and J. M. Baptista, *Meas. Sci. Technol.* **20**, 125201 (2009).

⁷S. Yin, P. B. Ruffin, and F. T. S. Yu, “Fiber Optic Sensors,” 2nd ed. (CRC, Boca Raton, 2008).

⁸A. D. Kersey and T. A. Berkoff, *IEEE Photon. Technol. Lett.* **4**(10), 1183–1185 (1992).

⁹E. Velosa, C. Gouveia, O. Frazão, P. A. S. Jorge, and J. M. Baptista, *IEEE Sens. J.* **12**(1), 201–206 (2012).

¹⁰B. T. Meggitt, W. Li, W. J. O. Boyle, and Y. M. Gebremichael, *J. Phys.: Conf. Ser.* **15**, 74–82 (2005).

¹¹G. A. Cranch, G. M. H. Flockhart, and C. K. Kirkendall, *J. Lightwave Technol.* **24**(4), 1787–1795 (2006).

¹²P. A. S. Jorge, L. A. Ferreira, and J. L. Santos, *Opt. Eng.* **39**(5), 1399–1404 (2000).

¹³P. L. Arens, *A Study on the Differential Thermal Analysis of Clays and Clays Minerals, Excelsiors Foto-Offset* (Excelsiors Foto-Offset, The Hague, 1951).

¹⁴E. S. Watson, M. J. O’Neill, J. Justin, and N. Brenner, *Anal. Chem.* **36**, 1233–1238 (1964).